

# Compositing “Stand Off” Ground Penetrating Radar Scans of Differing Frequencies

Roger Tilley, Hamid R. Sadjadpour, Farid Dowla

Department of Electrical Engineering  
University of California, Santa Cruz  
Santa Cruz, CA. 95064

Email: {rtvax, hamid, dowla} @soe.ucsc.edu

**Abstract**— Methods have been developed to combine signals of various frequencies in a manner to produce clearer images in the presence of noise. Ground Penetrating Radar (GPR) scans at various frequencies are no exception. Methods using an optimization problem solver, the Expectation-Maximization (EM) Algorithm, define weights used to perform the task of combining GPR scans. In this paper, we explore using the Gaussian Mixture Model (GMM) feature of the EM Algorithm on GPR scans taken at various heights above ground (“Stand Off” GPR). This method demonstrates the same measured improvement toward producing a cleaner image as GPR scans taken at ground level using the same EM Algorithm method.

**Keywords**-Ground Penetrating Radar; Expectation Maximization; Gaussian Mixture Model; Maximum Likelihood parameter estimation; Finite Difference Time Domain Method, GprMax.

## I. INTRODUCTION

Illuminating objects at various depths in a variety of terrains is the purview of Ground Penetrating Radar (GPR) scans. Different frequencies illuminate best at different depths. The higher the frequency the better illuminated the objects close to the surface are, with great fidelity. Conversely, the lower the frequency the better objects are illuminated at lower depths but with less detail. We previously examined, treating GPR scans at several frequencies, over the same area, like sub-components of a square wave. Where summing these sub-components, weighted by magnitude, created a square wave; suggesting that summing GPR Scans should form a crisper image to a lower depth than any one frequency scan. We reported that simply adding each scan together, as shown in [1][2], does not suffice. Summing weighted versions of each scan presents the best solution [1]. Determining the weights of each frequency scan provided the challenge. We were able to show that the EM Algorithm, an optimization problem solver, was an effective method for combining ground based GPR scans, using the data mixture feature [1]. What remains to be explored is whether the same is true for GPR scans at varying heights above the ground for the same buried objects and media, we previously examined [1].

In this paper, we explore the use of the Expectation Maximization (EM) Algorithm [3] in a role as an

optimization problem solver to determine the weights to be applied to each scan for an optimal weighted combination of scans. In Section II we discuss related work to combining GPR scans and processing them at varying heights. In Section III, we describe the EM data mixture process and its data mixture feature as it pertains to GPR scanned data.. In Section IV, we briefly cover the Maximum-Likelihood (ML) Estimation process as related to the EM Algorithm data mixture process [3][4]. In Section V, we present results of compositing of simulated GPR scan examples using the GprMax [5] software program to develop the individual GPR scans at various frequencies and transmitter/receiver heights above ground with buried targets in a defined media. In Section VI we draw conclusions and discuss future work.

## II. RELATED WORK

A literature search on compositing of GPR signals revealed only a few works. Papers on GPR time-slice analysis, overlay analysis and GPR isosurface rendering mostly by archaeologists; all similar in approach, were found. The technique was to illuminate the strongest reflections with a color or shading then combine the information by layers of depth, displaying the result [6].

For compositing of ground based GPR scans, work by Dougherty et al. [7] was the earliest found. Dougherty focused on methods to align each trace at its direct arrival peak, subtract the direct arrival pulse, and equalize the magnitude weight of each trace, then combine the traces. Booth et al. [8][9] confirmed Dougherty et al. [7] results and presented improved methods to develop frequency scan weighting techniques based on trace averaged amplitude spectra. Booth et al. [8][9] also proposed time invariant weighting methods consisting of matching the compositing results to an idealized amplitude spectrum output from a least-squares analysis.

Bancroft [10] introduced a double ramp summation method for computing weights. One ramp suppresses a frequency’s energy while another ramp increases an adjacent frequency’s energy all over time. The length of the ramp and start time was based on the wavelength of the frequency of interest. Weights developed as a ratio of the

average envelope of GPR frequencies was Bancroft's [10] additional contribution. Improvements over the previous works were minimal. This result is discussed in more detail in references [1][2].

A brief look at compositing of GPR scans at various heights revealed even less information. The literature at various heights was mostly concerned with Synthetic Aperture Radar (SAR) using single frequencies or chirped frequencies. The SAR literature focused on compensating for geometric distortion as the radar traversed the scan area; developing methods to piece the individual scans together. Other SAR papers [11][12][13] concerned themselves with accounting for phase shifts in the data from the angles the radar signals were sent and received from. Much discussion revolved around Gazdag [14], Stolt and FK migration [15] techniques. These techniques are beyond the scope of this paper and are part of future work discussions. Another SAR method discussed using Ultra-Wideband SAR radars to distinguish buried objects using an author developed "Method of Moments algorithm" [11].

Most, directly, related work focused on mathematically defining weights for each frequency by equal weighting, or defining weights that equalized the spectra of GPR frequencies through ramp summation, or a least squares process matching an idealized amplitude spectrum. Our previous work [1][2] explored GPR scans as a cluster mixture model problem using EM optimization problem solving methods for ground based scanned objects.

### III. EXPECTATION MAXIMIZATION ALGORITHM

To group like items contained in complex mixtures, or to solve incomplete data problems, or to determine membership weights of a collection of data points in a cluster, all are types of problems considered the purview of the EM Algorithm solution process. Our compositing of GPR scans process exploits this last feature, determining the membership weights in a cluster of data points within a Gaussian Mixture Model (GMM) [16][17]. The Gaussian distribution was chosen over other distributions because it is often used when the distribution of real-valued random variables is unknown.

We can define the EM Algorithm GMM process by first defining a finite mixture model,  $f(x;\theta)$ , of K components as mixtures of the following GMM function:

$$f(\underline{x}; \theta) = \sum_{k=1}^K \alpha_k p_k(\underline{x} | \theta_k), \quad (1)$$

Where:

- $p_k(\underline{x} | \theta_k)$  are K mixture components with a distribution defined over  $p(\underline{x} | \theta_k)$  with parameters  $\theta_k = \{\underline{\mu}_k, C_k\}$  (mean, covariance)
- $p_k(\underline{x} | \theta_k) =$

$$\frac{1}{(2\pi)^{d/2} |C_k|^{1/2}} e^{-\frac{1}{2}(\underline{x}-\underline{\mu}_k)^T C_k^{-1}(\underline{x}-\underline{\mu}_k)} \quad (2)$$

- $\alpha_k$  are K mixture weights, where  $\sum_{k=1}^K \alpha_k = 1$ .
- $\{\underline{x}_1, \dots, \dots, \underline{x}_N\}$  Data set for a mixture component in d dimensional space.

The EM Algorithm has 2 steps for each iteration. The first step is the Expectation step (E-step). The E-step determines the conditional expectation of the group membership weights ( $w_{ik}$ 's) for  $\underline{x}_i$ 's, introducing unobservable data based on  $\theta_k$ , the mean and covariance matrix. The second step is the Maximization step (M-step). New parameter values ( $\alpha_k, \underline{\mu}_k, C_k$ ); mixture weights, mean and covariance of weights; to maximize the finite mixture model are computed. The E-step and M-Step are repeated until convergence of the GMM model is reached. Convergence is characterized as the minimal change of the log-likelihood of the GMM function from one iteration to the next. The E-step and M-step equations are defined below:

E-Step –

$$w_{ik} = \frac{p_k(\underline{x}_i | \theta_k) \alpha_k}{\sum_{m=1}^K p_m(\underline{x}_i | \theta_m) \alpha_m} \quad (3)$$

for  $1 \leq k \leq K, 1 \leq i \leq N$ ;

with constraint  $\sum_{k=1}^K w_{ik} = 1$

M-Step –

$$N_k = \sum_{i=1}^N w_{ik} \quad (4)$$

$$\alpha_k^{new} = \frac{N_k}{N}, \text{ for } 1 \leq k \leq K \quad (5)$$

$$\underline{\mu}_k^{new} = \left(\frac{1}{N_k}\right) \sum_{i=1}^N w_{ik} * \underline{x}_i \quad (6)$$

for  $1 \leq k \leq K$

$$C_k^{new} =$$

$$\left(\frac{1}{N_k}\right) \sum_{i=1}^N w_{ik} * (\underline{x}_i - \underline{\mu}_k^{new})(\underline{x}_i - \underline{\mu}_k^{new})^T \quad (7)$$

Convergence (log likelihood of  $f(\underline{x}; \theta)$ ) –

$$\text{Log } l(\vartheta) =$$

$$\sum_{i=1}^N \log f(\underline{x}_i; \theta) =$$

$$\sum_{i=1}^N (\log \sum_{k=1}^K \alpha_k p_k(\underline{x}_i | \theta_k)) \quad (8)$$

These equations were implemented in MATLAB. The different scanning frequencies are represented by the variable 'k' and 'x' represents the GPR trace scans. Each trace, at a frequency and transmitter (Tx)/receiver (Rx)

position, are analyzed and combined for all frequencies before moving on to the next position. The EM GMM processing steps are briefly outlined below:

Expectation Maximization Gaussian Mixture Model process:

1. Initialize algorithm parameters; weights (mixture and group membership), mean, covariance, for each trace.
2. Expectation step – estimate parameters.
3. Maximization step – maximize estimated parameters.
4. Check for convergence – log likelihood of mixture model.
5. Repeat steps 2 – 4 until change from iteration to iteration is below or equal a defined value.
6. Combine traces with defined mixture weights.

#### IV. MAXIMUM LIKELIHOOD ESTIMATION PROCESS AND THE EM RELATIONSHIP

The EM algorithm provides a way to reduce a Maximum Likelihood Estimation (MLE) problem to a simpler optimization sub-problem, which is guaranteed to converge. This is the relationship between the MLE process and the EM algorithm. The MLE process provides an estimate of the unknown parameter, which maximizes the probability of getting the data we observed (likelihood).

An MLE process can be described as follows. Given a random sample  $X_1, X_2, \dots, X_n$ , independent and identically distributed (i.i.d.) with a probability density function  $f(x_i, \theta)$ , where  $\theta$  is the unknown parameter to be estimated; the joint probability density function (PDF) can be labeled as  $L(\theta)$ .

$$L(\theta) = P(X_1 = x_1, X_2 = x_2, \dots, X_n = x_n) = f(x_1; \theta) * f(x_2; \theta) \dots f(x_n; \theta) = \prod_{i=1}^n f(x_i; \theta) \quad (9)$$

Should the probability density function (PDF) be Gaussian with known variance  $\sigma^2$  and unknown mean,  $\mu$ , then, the likelihood equation becomes the following:

$$L(\mu) = \prod_{i=1}^n f(x_i; \mu, \sigma^2) = \sigma^{-n} (2\pi)^{-n/2} \exp\left(-\frac{1}{2\sigma^2} \sum_{i=1}^n (x_i - \mu)^2\right) \quad (10)$$

To determine the maximum value of the parameter  $\mu$ , for the likelihood equation, take the partial derivative of the log-likelihood equation with respect to (w.r.t.) the mean,  $\mu$ , and set the result equal to 0 and solve the remaining equation for the variable  $\mu$ . To determine if this value represents a maximum value for the likelihood equation, take the second partial derivative of the log-likelihood equation w.r.t.  $\mu$ ; should a negative value result, this verifies the parameter  $\mu$ , found is a maximum value for the likelihood function.

$$\text{Log}(L(\mu)) = -n \log(\sigma) - \frac{n}{2} \log(2\pi) - \sum_{i=1}^n \frac{(x_i - \mu)^2}{2\sigma^2} \quad (11)$$

$$\frac{\partial}{\partial \mu} (\log(L(u))) = -2(-1) \sum_{i=1}^n \frac{(x_i - \mu)}{2\sigma^2} = 0 \quad (12)$$

$$\text{Solve for } \mu; \quad \mu = \frac{\sum_{i=1}^n x_i}{n} \quad (13)$$

Second derivative –

$$\frac{\partial^2}{\partial \mu} (\log(L(u))) = \sum_{i=1}^n \frac{(-1)}{\sigma^2} = -\frac{n}{\sigma^2} \quad (14)$$

The second derivative is negative; by definition the calculated  $\mu$  value is a maximum.

When there are at least two sets of data, one partially observed (hidden), or when mixture parameters are to be estimated, the MLE process becomes hard. For example, a mixture distribution of the form  $f(x) = \sum_{k=1}^K \alpha_k f(x; \theta_k)$ , where there are K number of components in the mixture model and for each k, there is a PDF,  $f(x; \theta_k)$  with weights  $\alpha_k$  and a complete observed data set  $x$  with additional constraints  $\sum_k \alpha_k = 1$  and  $\alpha_k \geq 0$  for all k; the joint PDF has the following form with  $n$  observed data for each k:

$$L(x|\alpha, \theta_k) = \prod_{i=1}^n \sum_{k=1}^K \alpha_k f(x_i; \theta_k) \quad (15)$$

The log of the likelihood equation is as follows:

$$\text{Log}((L(x|\alpha, \theta_k))) = \sum_{i=1}^n \log \sum_{k=1}^K \alpha_k f(x_i; \theta_k) \quad (16)$$

Using MLE to solve this equation presents a challenge to determine the derivative of the log of sums and the start value for the weight,  $\alpha_k$ , associated with an individual distribution. Many local maxima can be found that are less than the global maximum, calculated using an established value of  $\alpha_k$ . Selecting the weight value that attains the global maximum for the above log-likelihood equation is not likely in short order.

The EM algorithm process provides a method to estimate the weights, guarantee convergence of the log-likelihood equation [3][4] to a non-decreasing local maximum with each completion of all steps outlined in Section II. A feature of the EM algorithm is that each local maximum achieved increases toward a global maximum. The E-step uses existing values to calculate the probability of weight start values. The M-step recalculates the model parameters then, calculates the maxima for that set of parameters using the MLE process. The EM algorithm reduces the MLE optimization problem to a sequence of simpler optimization sub-problems, each guaranteed to converge. The EM process is repeated until a global maximum is reached.

The EM algorithm incorporates the MLE process only after reducing the model to a form, which is guaranteed to converge. To combine GPR frequency scans, the actual weights of each frequency scan are unknown or hidden. The manner the EM algorithm uses to accomplish workable solutions to hidden or incomplete data, makes a distinction from other optimization problem solvers; as a result, making

it a featured candidate to provide a solution to combining multiple GPR frequency scans.

### V. GPR SCAN RESULTS

We examine extending the capability of the EM GMM problem solver by using the defined model areas from our previous work [1][2]. Areas were defined using the Finite Difference Time Domain (FDTD) [18] modeling software package GprMax by A. Giannopoulos [5] to create GPR scans in various media. 3-D hardware verification of the software was determined in reference [19], but only 2-D analyses were performed here. Examples were constructed such that the Transmitter (Tx) and Receiver (Rx) heights above the ground were changed for each EM GMM in-depth analysis. Tx/Rx heights examined included 5 meters, 10 meters, 20 meters and 40 meters.

The first defined area modeled consisted of Tx/Rx suspended 5 meters above the ground in air [1], repeated here for continuity in our discussion of height effects on EM GMM problem solver. The target (a perfect electrical conductor) is buried 10 meters below the surface in a moist-sand medium with relative permittivity ( $\epsilon_r$ ) of 9.0, and an electrical conductivity of 0.001 mS/m (milli-Siemens per meter) (Simulated Analysis 1 – SA1). The target is 2 meters length and 0.5 meters in depth. Each Tx/Rx is moved along the scan axis (x – axis) 0.25 meters per step for a total of 36 scans. The model area is 10 meters in width and 25 meters in depth. The Tx position starts at 0.5 meters ending at 9.5 meters, and the Rx position starts at 0.75 meters ending at 9.75 meters. Each scan is 425 ns in length, long enough to receive a reflected signal 24 meters below a Tx/Rx in the medium of air and moist-sand. The defined model has a minimum grid space of 200 points in the x direction, ( $\Delta x - 0.05$  meters), and 500 points in the y-direction, ( $\Delta y - 0.05$  meters). Figure 1 shows the model, Tx/Rx positions and target area.

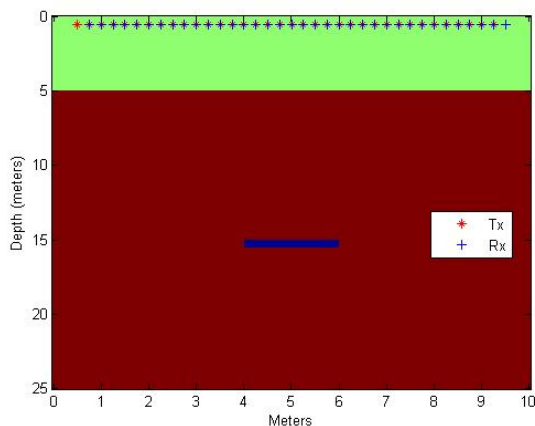


Figure 1. Defined Space with buried target at 15 meters depth and Tx's & Rx's 5 meters above ground.

Six frequency scans were calculated for model SA1. Scans at 20, 30, 50, 100, 500 and 900 MHz were combined using the EM GMM problem solver to determine the weights of each scan. Figure 2 shows the signals combined by scaling each signal max value to the same magnitude with the direct arrival and ground bounce signals removed. The target reflection is a broad area roughly 240 ns to 320 ns in depth (two-way travel time); a coarse indication of the depth of the target. The direct arrival signal is a signal that travels directly (line of sight) from a Tx to an Rx. A ground bounce signal is a radar return from the ground. The direct arrival signal was removed by subtracting a GPR scan without a target from a scan with a target, for each frequency. A broad area of target reflection is shown from approximately 240 ns to 320 ns in depth (two-way travel time); a very rough indication of target depth.

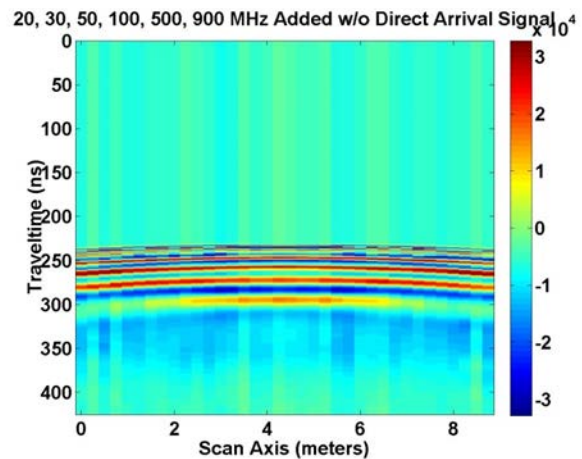


Figure 2. Sum of frequency signals with direct arrival and ground bounce signals removed.

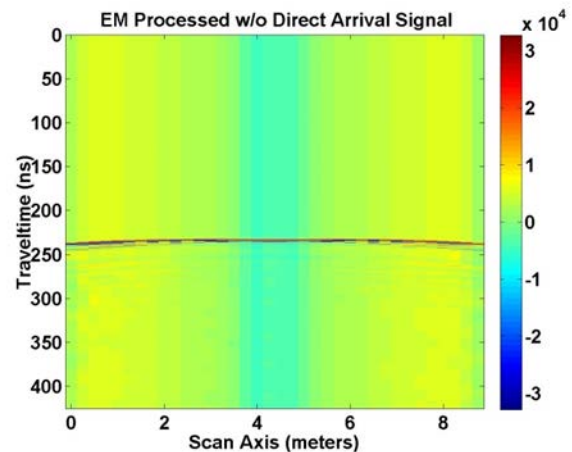


Figure 3. EM sum of frequency signals with Direct Arrival and ground bounce signals removed.

Figure 3 shows the result of EM processed combined signals with the direct arrival and ground bounce signals removed. The target is correctly depicted at 10 meters below ground, approximately 15 meters below Tx's and Rx's (240 ns). The improvement of defining scan weights using the

EM Algorithm process is clearly visible. However, the Figure shows a broadened output result; broader than the target. This is attributed to the fact that the model is more like a bore hole; area twice as deep as its width. This and the inclusion of lower frequencies in the sum, account for the reverse “u-shaped” area beginning at the target depth outward.

Though the model created a bore hole effect, analysis continued for heights of 10, 20 and 40 meters above the ground with the same width model to judge whether the target would be revealed at the correct depth ignoring the target width that might be displayed. Figures 4–9 depict the model and the output result of combining 6 frequencies (20, 30, 50, 100, 500 and 900 MHz), using the EM algorithm to define the weights of each scan for each of the remaining 3 heights.

Figure 4 and Figure 5 depict the simulated analysis model and ground penetrating radar response when the Tx/Rx height is 10 meters above the ground. The target is correctly depicted at 20 meters (270 ns – two-way travel time) below Tx’s and Rx’s.

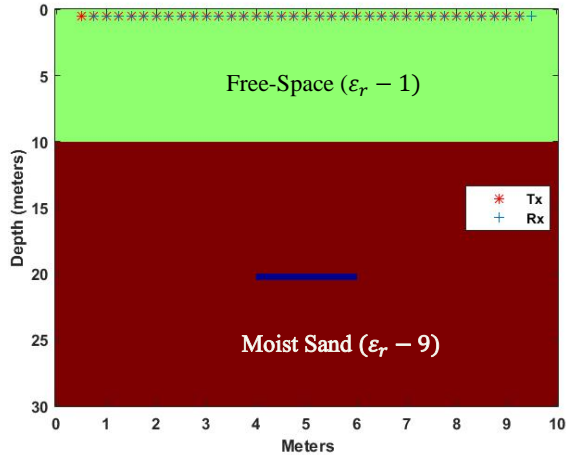


Figure 4. Defined Space of SA1, with buried target at 20 meters depth from Tx’s & Rx’s 10 meters above ground.

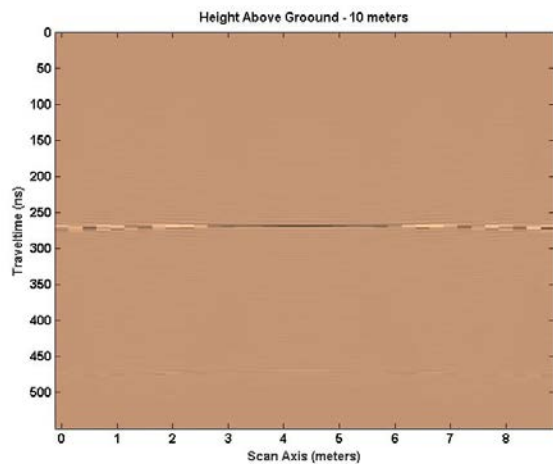


Figure 5. Output response of SA1, EM sum of frequency signals with Direct Arrival and ground bounce signals removed.

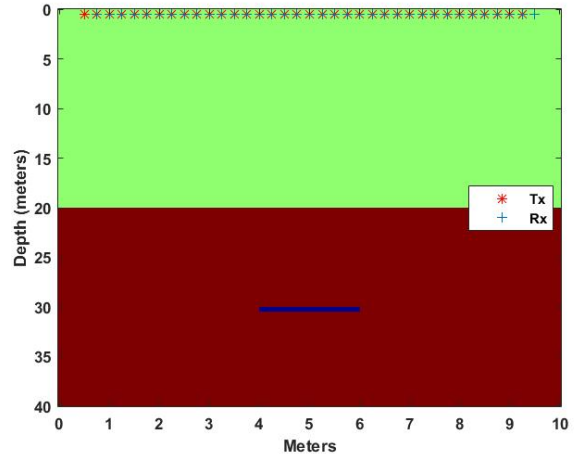


Figure 6. Defined space of SA1, with buried target at 30 meters from Tx’s & Rx’s 20 meters above ground.

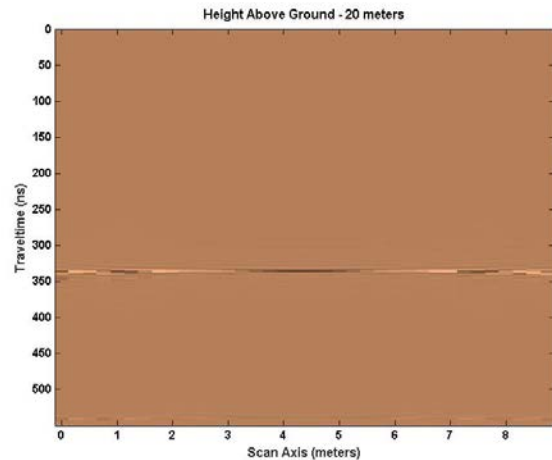


Figure 7. Output response of SA1, EM sum of frequency signals with Direct Arrival and ground bounce signals removed.

The simulated analysis of model SA1 was repeated for Tx/Rx heights of 20 meters above the ground (Figure 6) and 40 meters above ground (Figure 8). The target is depicted at 30 meters (335 ns) in Figure 7 and 50 meters (468 ns) in Figure 9 from the Tx’s and Rx’s, as expected for two-way travel times.

A second defined space model; (Simulated Analysis 2 – SA2) was developed to examine EM Algorithm response to a slightly different model type (Figure 10.). SA2 consists of an area 30 meters in length and 25 meters in depth. Four cases of Tx/Rx heights above the ground were analyzed. Cases included Tx/Rx at 5, 10, 20, and 40 meters above the ground. As before, a Tx/Rx combination is swept along the x direction axis beginning at 0.5 meters ending at 29.85 meters with Tx/Rx spacing of 0.25 meters. The number of GPR scans is 145 with a minimum grid space of 150 points in the x direction, ( $\Delta x - 0.2$  meters) and 2500 points in the y direction, ( $\Delta y - 0.01$  meters), dependent on the height above ground. The space above ground was defined as free-space with relative permittivity ( $\epsilon_r$ ) of 1.0 and electrical

conductivity of 0 mS/m or lossless. The scanned medium is dry-sand with a relative permittivity ( $\epsilon_r$ ) of 3.0 and electrical conductivity of 0.01 mS/m.

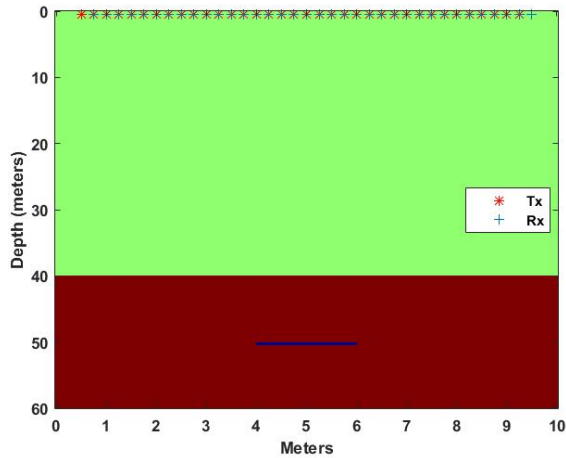


Figure 8. Defined Space of SA1, with buried target at 50 meters depth from Tx's & Rx's 40 meters above ground.

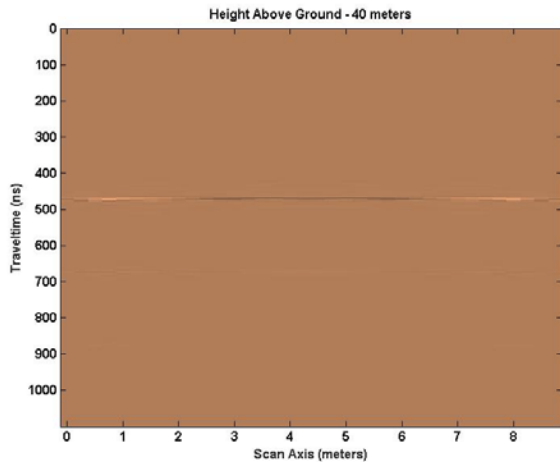


Figure 9. Output Response of SA1, EM sum of frequency signals with Direct Arrival and ground bounce signals removed.

Buried in the ground at 8 different levels (4.565, 6.065, 8.565, 10.065, 12.815, 14.065, 16.565 and 18.065 meters) are sheets modelled as perfect electrical conductors [1][2]. Each sheet is 2 meters in length and 0.1 meter thick. The scanning frequencies are the same as previously noted, (20, 30, 50, 100, 500 and 900 MHz). Figure 10, Figure 12, Figure 14 and Figure 16 show the four SA2 models for Tx/Rx heights above ground (5, 10, 20 and 40 meters) and the simulated sheets of corrugated aluminum modelled as perfect electrical conductors. References [1][2], used the same model with the exception that the Tx's and Rx's were just barely above ground. Figure 11, Figure 13, Figure 15, Figure 17 and Figure 18 display the GPR response after being processed using the EM GMM algorithm. Figure 18 displays the individual GPR traces instead of the image response. The direct arrival and ground bounce signal have been removed by subtraction in each case. At each height 8 sheets are depicted though their outline is not very clear and

worsens as the height increases. At 40 meters, only the individual trace response designates the 8 sheets.

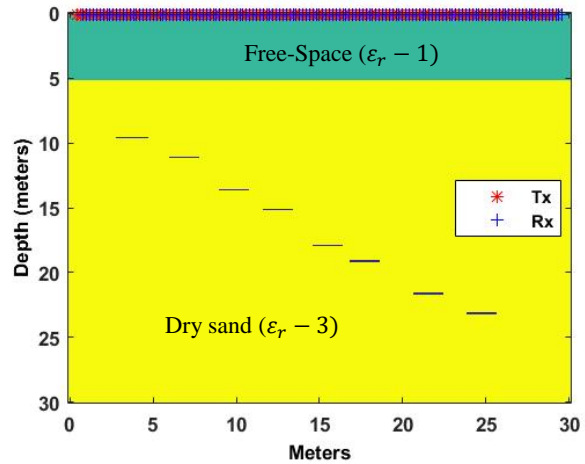


Figure 10. Defined Space of SA2, (8) 2 meter long plates, 0.1 meter thick with Tx's & Rx's 5 meters above ground.

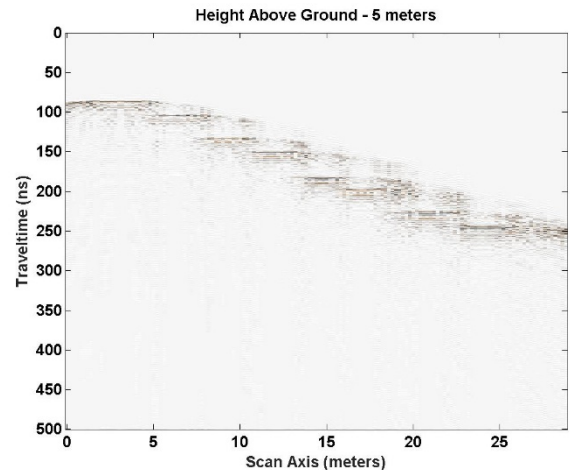


Figure 11. Output response of SA2, EM sum of frequency signals with Direct Arrival and ground bounce signals removed.

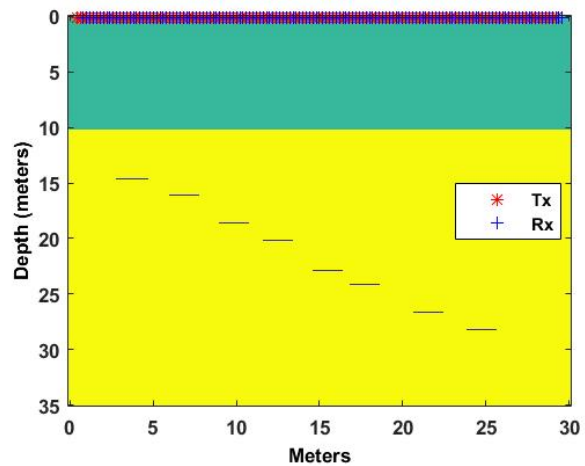


Figure 12. Defined Space of SA2, (8) 2 meter long plates, 0.1 meter thick with Tx's & Rx's 10 meters above ground.

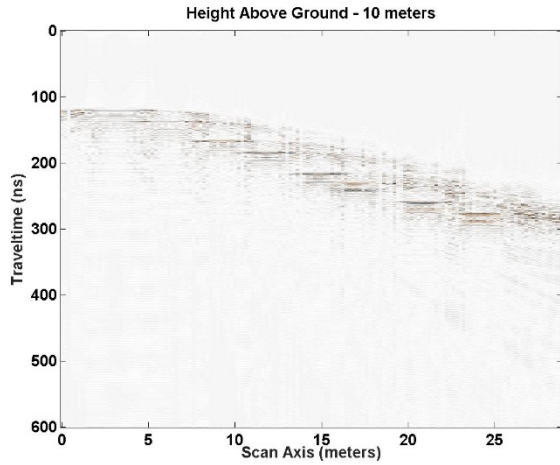


Figure 13. Output response of SA2, EM sum of frequency signals with Direct Arrival and ground bounce signals removed.

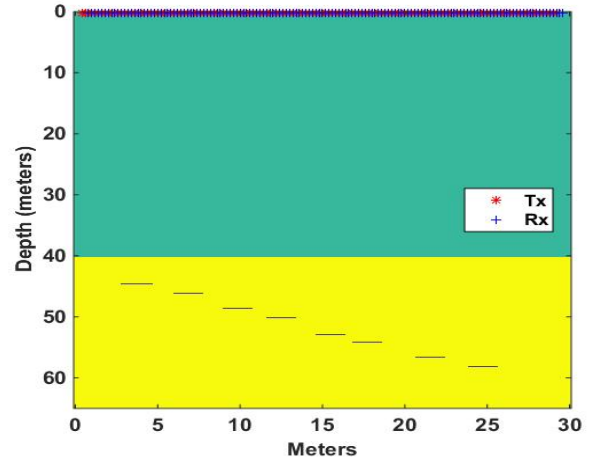


Figure 16. Defined Space of SA2, (8) 2 meter long plates, 0.1 meter thick with Tx's & Rx's 40 meters above ground.

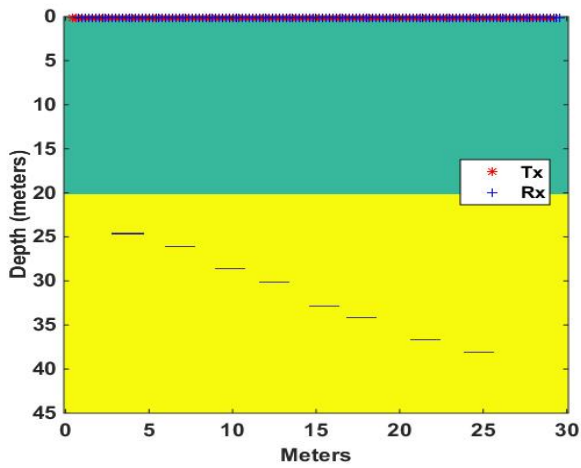


Figure 14. Defined Space of SA2, (8) 2 meter long plates, 0.1 meter thick with Tx's & Rx's 20 meters above ground.

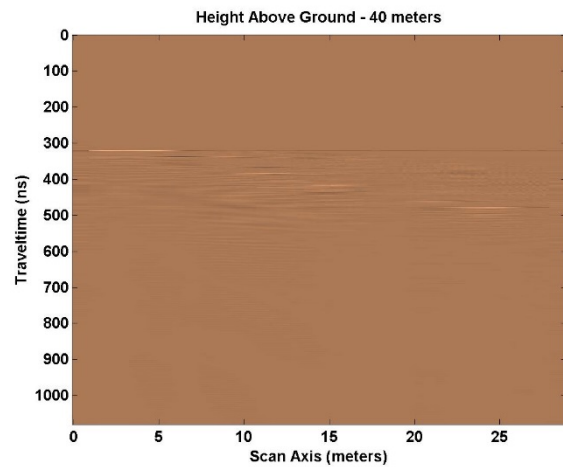


Figure 17. Output response of SA2, EM sum of frequency signals with Direct Arrival and ground bounce signals removed.

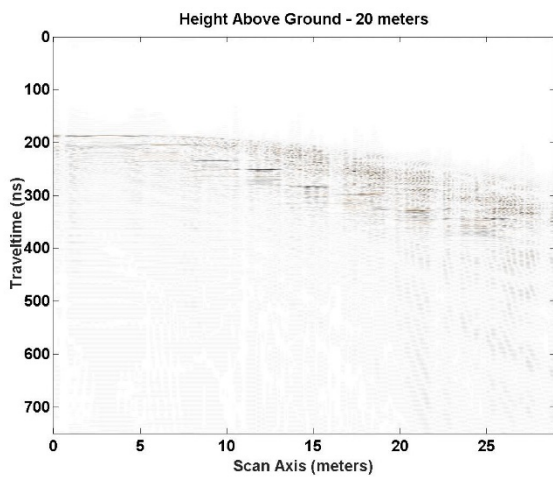


Figure 15. Output response of SA2, EM sum of frequency signals with Direct Arrival and ground bounce signals removed.

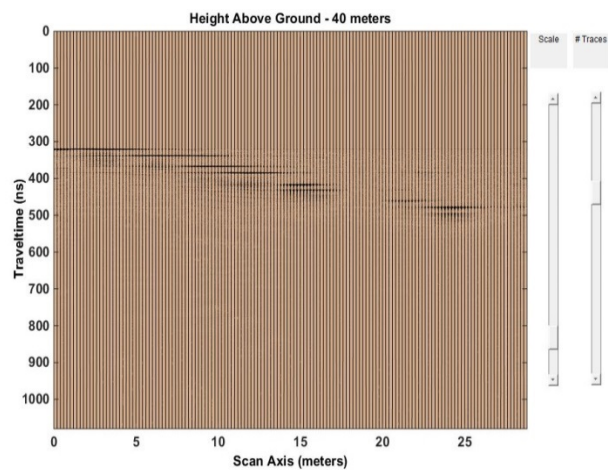


Figure 18. Signal traces of SA2 output response of EM sum of frequency signals with Direct Arrival and ground bounce signals removed.

A third defined space model, Simulated Analysis 3 (SA3), was designed to examine the response of EM GMM algorithm on a defined space where the media is non-uniform. SA3 contains corrugated aluminum sheets modelled as perfect electrical conductors in dry sand, clay, granite, concrete and limestone media (Figure 19). The relative permittivity of each medium is noted in same figure. The details of the model are the same as SA2 except for the media used. Figure 19, Figure 21, Figure 23 and Figure 25 display the model with Tx's and Rx's at 4 different heights. Tx/Rx heights are 5, 10, 20, 40 meters above ground. GPR scanning frequencies are 6 total, 20, 30, 50, 100, 500, and 900 MHz. Figure 20, Figure 22, Figure 24, Figure 26 and Figure 27 depict the response to the GPR scans processed using the EM GMM process. The direct wave and ground bounce reflected signals have been removed by subtraction. As the Tx/Rx height above ground increases, locating the 8 sheets in the image is less clear, but they can be found. At the 40 meter height, the best depiction of all 8 sheets is the display of individual EM processed GPR signal traces (Figure 27) rather than the image response.

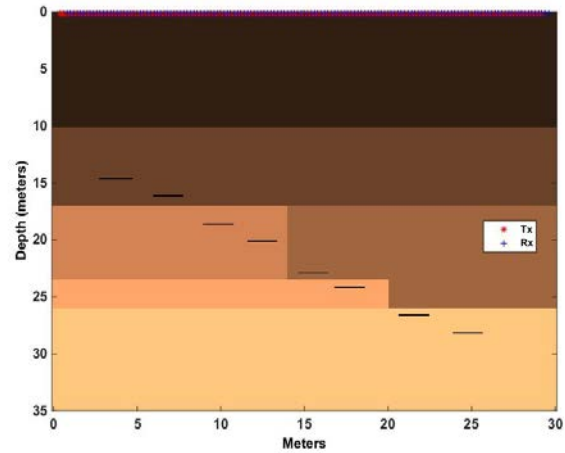


Figure 21. Defined Space of SA3, (8) 2 meter long plates, 0.1 meter thick with Tx's & Rx's 10 meters above ground

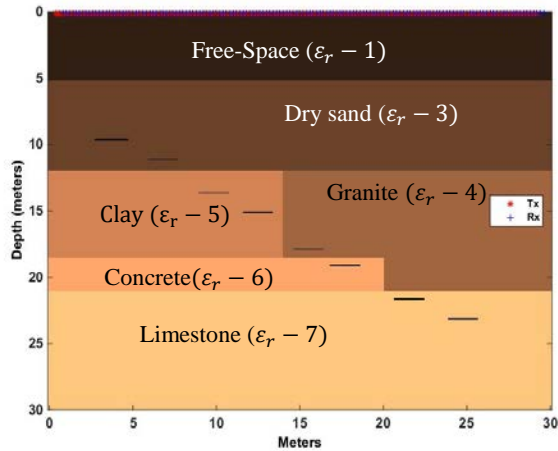


Figure 19. Defined Space of SA3, (8) 2 meter long plates, 0.1 meter thick with Tx's & Rx's 5 meters above ground.

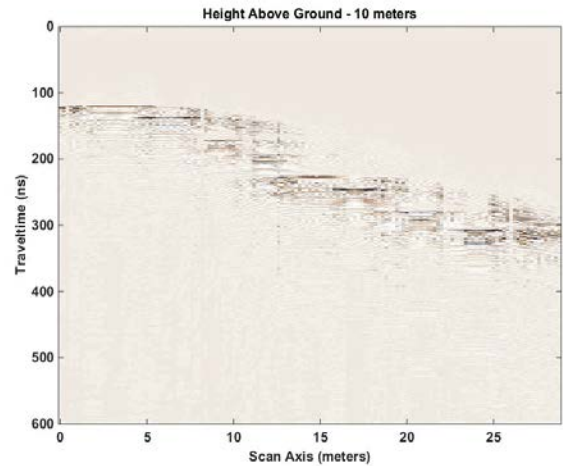


Figure 22. Output response of SA3, EM sum of frequency signals with Direct Arrival and ground bounce signals removed.

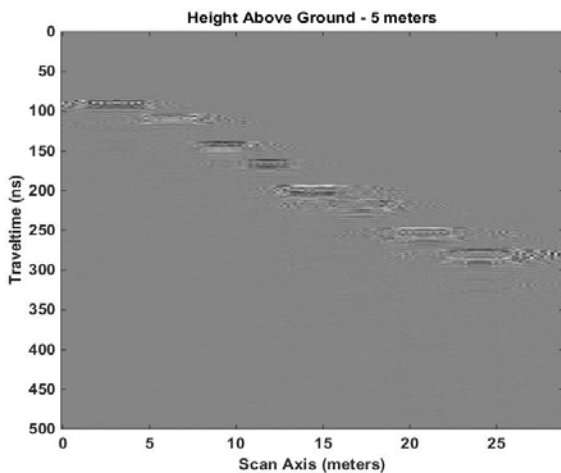


Figure 20. Output response of SA2, EM sum of frequency signals with Direct Arrival and ground bounce signals removed.

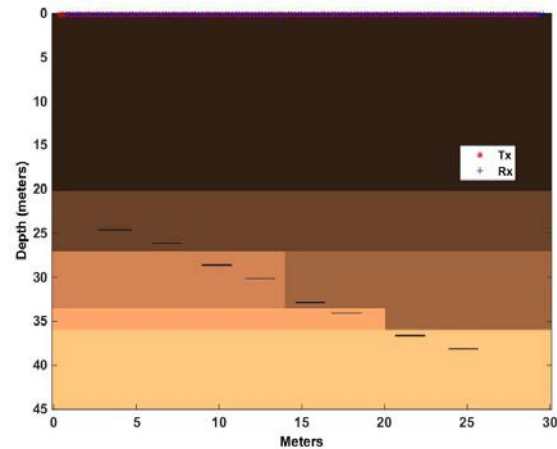


Figure 23. Defined Space of SA3, (8) 2 meter long plates, 0.1 meter thick with Tx's & Rx's 20 meters above ground.



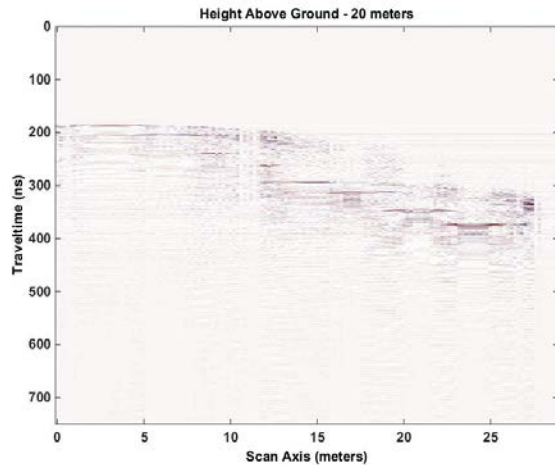


Figure 24. Output response of SA3, EM sum of frequency signals with Direct Arrival and ground bounce signals removed.

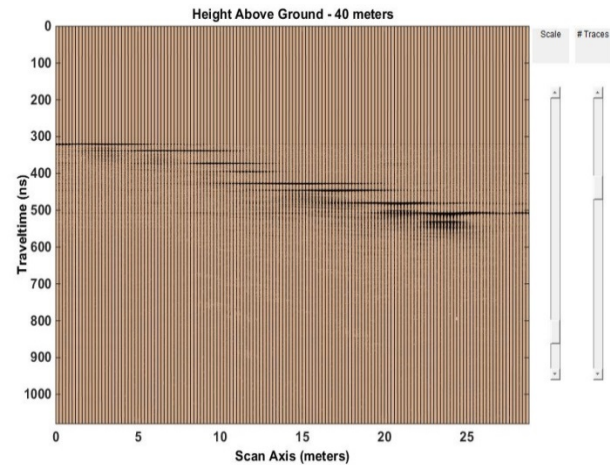


Figure 27. Signal traces of SA3 output response of EM sum of frequency signals with Direct Arrival and ground bounce signals removed.

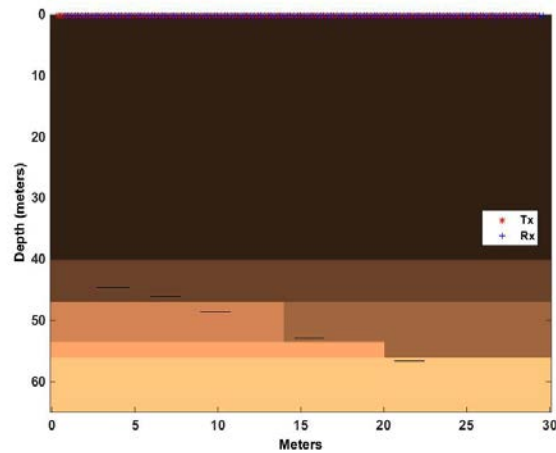


Figure 25. Defined Space of SA3, (8) 2 meter long plates, 0.1 meter thick with Tx's & Rx's 40 meters above ground

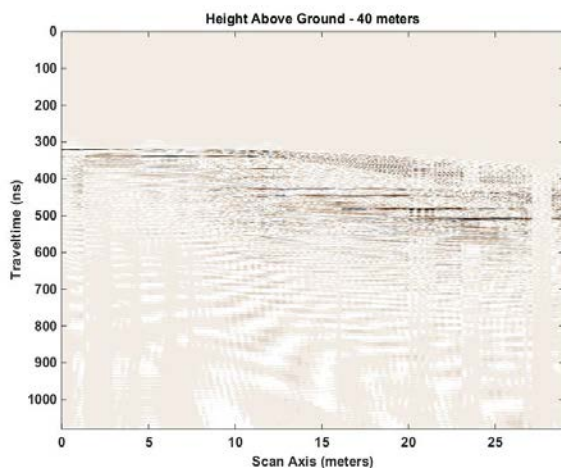


Figure 26. Output response of SA3, EM sum of frequency signals with Direct Arrival and ground bounce signals removed.

## VI. CONCLUSION AND FUTURE WORK

In this paper, as an extension of reference [1], we explored the use of the Expectation Maximization Gaussian Mixture Model method [3] to combine multiple frequency scans of the same target area. We examined the effectiveness of the EM GMM method on ground Penetrating Radar scans using transmitter and receiving antennas placed at various heights over the same target areas and media types as described in reference [1]. We conducted the analyses using the software program GprMax [5] due to the lack of actual hardware, real areas to scan and to compare results with reference [1] examples. Actual 3-D hardware verification of the GprMax software was determined in reference [19].

As part of the related work discussion, we reviewed the Maximum Likelihood Estimation process and its problem of working with hidden or incomplete data [3][4]. When hidden or incomplete data exists, a closed form solution of the MLE equation or a single global maximum is not easily obtained and very hard to solve for. We reviewed the EM GMM algorithm process and its benefit of working easily with hidden or incomplete data; creating a set of optimization problems simpler and guaranteed to converge while ultimately producing a global maximum after several iterations of producing increasing local maxima. We also, briefly reviewed other methods of compositing found in the literature. Methods of Dougherty et al. [7], Booth et al. [8][9] and Bancroft [10] we found to be less effective than our EM GMM method of reference [2]. Lastly, we found in the literature that scanning from various heights has been the purview of Synthetic Aperture Radars. SAR technology information obtained [11][12][13] did not concern itself with compositing but, did research methods to stitch area scans together, account for phase shifts [14][15] in the data, due to scanning angles, and distinguish objects with an author developed "Method of Moments Algorithm" [11].

Using GprMax [5], we repeated scanning the same test areas using the same 6 frequencies (20, 30, 50, 100, 500, and 900 MHz) as our previous work at 5, 10, 20 and 50 meters above ground. Our method performed well with outcomes similar to our previous results of scans with Tx's and Rx's near the ground. Images at heights above 20 meters were a challenge to recognize independent of the media that surrounding the targets. Moist sand, dry sand, concrete, clay granite and limestone did not change the end resulting image perceptibly. The method used to remove the direct wave/ground bounce signal also removed the boundary reflections for non-homogenous media. The test areas were scanned with the media and targets in place; then re-scanned with media in place without the targets. The scan with media and targets was subtracted from the scan with media without targets.

Problem areas remaining to be addressed are edge detection capability, removal of direct wave/ground bounce without removal of the reflected target responses, alignment of GPR trace starting points across frequencies and accounting for phase-shifts in the data. The SAR method solution was to use Gazdag [14] or F-K migration [15] techniques to manage phase-shifts in the data. We are encouraged that these methods will address the edge detection problem favorably.

#### ACKNOWLEDGMENT

This work was performed under the auspices of Sandia National Laboratories a multimission laboratory managed and operated by National Technology and Engineering Solutions of Sandia, LLC, a wholly owned subsidiary of Honeywell International, Inc. for the U.S. Department of Energy's National Nuclear Security Administration under contract DE-NA-0003525.

#### REFERENCES

- [1] R. Tilley, H. Sadjadpour, and F. Dowla, "Combining Ground Penetrating Radar Scans of Differing Frequencies Through Signal Processing," The Ninth International Conference on Advanced Geographic Information Systems, Applications, and Services, GEOProcessing 2017, Nice, France, Mar 2017, pp. 32-38, ISBN:978-1-61208-539-5.
- [2] R. Tilley, H. Sadjadpour, F. Dowla, "Compositing Ground Penetrating Radar Scans of Differing Frequencies for Better Depth Perception", International Journal on Advances in Software, vol. 10, no. 3 & 4, year 2017, pp 413-431, ISSN 1942-2628. <https://www.iariajournals.org/software/tocv10n34.html>, 2018.7.30
- [3] A. P. Dempster, N.M. Laird and D.B. Rubin, "Maximum Likelihood from Incomplete Data via the EM Algorithm," Journal of the Royal Statistical society, Series B (Methodological) 39(1): pp. 1-38, 1977, JSTOR 2984875.MR0501537.
- [4] C. R. Shalizi, "Advanced Data Analysis from an Elementary Point of View," Book Draft from Lecture Notes for Course 36-402 at Carnegie Mellon University, Chapters 19.1-19.2.2, January 2017. <http://www.stat.cmu.edu/~cshalizi/ADAfaEPoV/ADAfaEPoV.pdf>, 2017.11.23.
- [5] A. Giannopoulos, "Modelling Ground Penetrating Radar by GprMax," Construction and Building Materials, vol. 19, pp. 755-762, Dec 2005, DOI 10.1016/j.conbuildmat.2005.06.007.
- [6] J. A. Pena, and T. Teixido, "Cover Surfaces as a New Technique for 3-D Image Enhancement, Archaeological Applications," Repositorio Institucional de la Universidad de Granada, Spain, 2012, <http://hdl.handle.net/10481/22949>, 2017.11.23.
- [7] M. E. Dougherty, P. Michaels, J. R. Pelton, and L. M. Liberty, "Enhancement of Ground Penetrating Radar Data Through Signal Processing," Symposium on the Application of Geophysics to Engineering and Environmental Problems 1994, pp. 1021-1028, Jan 1994, DOI 10.4133/1.2922053.
- [8] A. L. Endres, A. Booth, and T. Murray, "Multiple Frequency Compositing of Spatially Coincident GPR Data Sets," Proceedings of the Tenth International Conference on Ground Penetrating Radar, 2004, Delft, The Netherlands, June 2004, pp. 271-274, ISBN: 90-9017959-3.
- [9] A. D. Booth, A. L. Endres, and T. Murray, "Spectral Bandwidth Enhancement of GPR Profiling Data Using Multiple-Frequency Compositing," Journal of Applied Geophysics, vol 67, pp. 88-97, Jan 2009, DOI 10.1016/j.jappgeo.2008.09.015.
- [10] S. W. Bancroft, "Optimizing the Imaging of Multiple Frequency GPR Datasets using composite Radargrams: An Example from Santa Rosa Island, Florida," PhD dissertation, University of South Florida, 2010.
- [11] S. Vitebskiy, L. Carin, and M. Ressler, "Ultra-Wideband, Short-Pulse Ground-Penetrating Radar: Simulation and Measurement," IEEE Transactions on Geoscience and Remote Sensing, Vol. 35, NO. 3, May 1997, pp. 762-772. <https://www.math.ucdavis.edu/~saito/data/sonar/vitebskiy.pdf>, 2018.7.30.
- [12] M. Skjelvareid, "Synthetic aperture ultrasound imaging with application to interior pipe inspection", PhD dissertation, University of Tromso, 2012. ISBN 978-82-8236-067-8, <http://hdl.handle.net/10037/4649>, 2018.7.30.
- [13] H. Zhang, W. Benedix, D. Plettemeier, and V. Ciarletti, "Radar Subsurface Imaging by Phase Shift Migration Algorithm," 2013 European Microwave Conference, Nuremberg, 2013, pp. 1843-1846. DOI: 10.23919/EuMC.2013.6687039. <https://ieeexplore.ieee.org/iel7/6679726/6686544/06687039.pdf>, 2018.7.30.
- [14] J. Gazdag, "Wave Equation with the phase-shift method", Geophysics, Vol. 43, NO. 7, December 1978, pp. 1342-1351. DOI: 10.1190/1.1440899. <https://doi.org/10.1190/1.1440899>, 2018.7.30
- [15] R. Stolt, "Migration by Fourier Transform", Geophysics, Vol. 43, NO. 1, February 1978, pp 23-48. DOI: 10.1190/1.1440826. <https://www.math.ucdavis.edu/~saito/data/sonar/stolt.pdf>, 2018.7.30.
- [16] Padhraic Smyth, "The EM Algorithm for Gaussian Mixtures, Probabilistic Learning: Theory and Algorithms, CS274A," University of California, Irvine, Department of Computer Science, Lecture Note 4.
- [17] J. J. Verbeek, N. Vlassis, and B. Kröse, "Efficient Greedy Learning of Gaussian Mixtures," The 13th Belgian-Dutch Conference on Artificial Intelligence (BNAIC'01), pp. 251-258, 2001, INRIA-00321510.
- [18] A. Tavlove, "Review of the formulation and Applications of the Finite-Difference Time-Domain Method for Numerical Modeling of Electromagnetic-Wave Interactions with Arbitrary Structures," Wave Motion, vol. 10, pp. 547-582, Dec 1988, DOI 10.1016/0165-2125(88)90012-1.

- [19] R. Tilley, F. Dowla, F. Nekoogar, and H. Sadjadpour, "GPR Imaging for Deeply Buried Objects: A Comparative Study Based on FDTD models and Field Experiments", Selected Papers Presented at the MODSIM World 2011 Conference and Expo; pp. 45-51, 2012; (NASA/CP-2012-217326); (SEE 20130008625).  
<https://ntrs.nasa.gov/archive/nasa/casi.ntrs.nasa.gov/20130008669.pdf>, 2018.11.13.